Journal of Organometallic Chemistry 733 (2013) 63–70

Contents lists available at SciVerse ScienceDirect

Journal of Organometallic Chemistry

journal homepage: www.elsevier.com/locate/jorganchem

Photosensitive iron(II)-based CO-releasing molecules (CORMs) with vicinal amino and diphenylphosphino substituted chelating ligands

Taghreed M.A. Jazzazi [a], Helmar Görls [a], Guido Gessner [b], Stefan H. Heinemann [b], M. Westerhausen [a,*]

[a] Institute of Inorganic and Analytical Chemistry, Friedrich Schiller University Jena, Humboldtstraße 8, 07743 Jena, Germany
[b] Center for Molecular Biomedicine, Department of Biophysics, Friedrich Schiller University Jena & Jena University Hospital, Germany

ARTICLE INFO

Article history:
Received 27 November 2012
Received in revised form
8 February 2013
Accepted 13 February 2013

Keywords:
CO release
CORM
Iron
Iron carbonyl complexes
Myoglobin–CO assay
Photo-CORM

ABSTRACT

The reactions of $[Fe(H_2O)_6]$ $[BF_4]_2$ with aminoethyl-diphenylphosphane and 2-(diphenylphosphino)aniline lead to the formation of *trans*-$[Fe(NC\text{-}Me)_2(H_2NCH_2CH_2PPh_2)_2]$ $[BF_4]_2$ (**1a**) and *trans*-$[Fe(NC\text{-}Me)_2(H_2NC_6H_4\text{-}2\text{-}PPh_2)_2]$ $[BF_4]_2$ (**1b**), respectively. One acetonitrile ligand can be substituted by CO yielding $[Fe(CO)(NC\text{-}Me)(H_2NCH_2CH_2PPh_2)_2]$ $[BF_4]_2$ (**2a**, CORM-P1) and $[Fe(CO)(NC\text{-}Me)(H_2NC_6H_4\text{-}2\text{-}PPh_2)_2]$ $[BF_4]_2$ (**2b**, CORM-P2). Upon irradiation with visible light, CO is liberated making especially **2a** a promising photo-CORM whereas for **2b** a slow and incomplete CO release is observed.

Carbon monoxide, an important signaling molecule [1–3] with a huge therapeutic potential [4–6], is mostly formed during heme degradation together with iron(II) ions [7]. However, CO also expresses a well-known toxicity and exhibits poor solubility and lack of selectivity – all aspects hampering the use of gaseous carbon monoxide as a therapeutic agent. Therefore, carriers have to be used for targeting carbon monoxide to cells and tissues. Such carriers have to fulfill certain prerequisites such as non-toxicity of themselves as well as their degradation products after CO release, adequate solubility and stability in water, and a mode of CO release that can be triggered by ligand substitution reactions, pH or temperature changes, enzymes, or by visible light. Metal carbonyl complexes are appropriate carriers for CO [8,9] and represent a promising class of future pharmaceuticals as CO-releasing molecules (so-called CORMs). Especially metal carbonyl complexes that liberate CO upon radiation with visible light (photo-CORMs) recently gained particular interest [10–13]. According to the importance and the enormous expectations with respect to clinical benefits several recent review articles summarize the strategies and medicinal aspects of carbon monoxide treatments [14–16].

In medicinal applications the effects of potentially toxic breakdown products have to be considered. Iron-based CORMs represent a promising substance class because iron(II) is a non-toxic 3d metal whose concentration is effectively regulated in biological systems [17]. Therefore, many investigations focused on iron-based carbonyl complexes and date back several decades. More than eighty years ago, Cremer demonstrated that iron complexes with biogenic cysteine and isocysteine ligands reversibly bind carbon monoxide [18,19]. The possibility of triggering CO liberation from iron carbonyl complexes with visible light was discovered very early, too [20]. The iron carbonyl complexes with chelating cysteine and cysteamine ligands were used to study the oxidation state of iron in its enzymes [21,22]. Thereafter, numerous research groups investigated synthesis, physical behavior, and chemical reactivity of iron(II) carbonyl complexes containing thiolates with S/N-donor pairs (see for example Refs. [23–32]). In these complexes the carbonyl molecules are *cis*-arranged with the nitrogen donor atoms in trans-positions. The compound class of iron(II)-based CORMs also includes thiolates (e.g. Refs. [33,34]), multidentate amines (e.g. Refs. [35,36]), dithiocarbamates [37], and even π-bonded unsaturated hydrocarbons (e.g. Refs. [38–41]).

The activity of CORMs is commonly measured by a myoglobin assay in a buffered solution containing deoxymyoglobin (Mb) with excess of sodium dithionite. In this test, liberated carbon monoxide reacts with Mb to myoglobin–CO complex (Mb–CO) and the amount of Mb–CO formed is quantified spectroscopically. This test causes challenges when the CORMs show an intense color and, hence, requires a modified analysis of the spectroscopic data [42].

* Corresponding author. Tel.: +49 3641 948110; fax: +49 3641 948102.
E-mail address: m.we@uni-jena.de (M. Westerhausen).

0022-328X/$ – see front matter © 2013 Elsevier B.V. All rights reserved.
http://dx.doi.org/10.1016/j.jorganchem.2013.02.015

In addition, it was observed that the sulfite species enhance CO liberation in Ru-based CORM-2 ($[Ru(CO)_3Cl_2]_2$) and CORM-3 ($[Ru(CO)_3Cl(glycinate)]$), which release carbon monoxide via a ligand substitution mechanism [43].

In the course of our investigations of iron(II)-based CORMs we compared dicarbonyl-*bis*(cysteaminato)iron(II) (CORM-S1) and dicarbonyl-*bis*(ortho-aminothiophenolato)iron(II) (CORM-S2). In CORM-S2, a step-wise CO release was observed upon irradiation with visible light whereas both carbon monoxide molecules were liberated at the same time from CORM-S1. Here, we intended to investigate an iron(II)-based photo-CORM with only one CO ligand coordinated to the metal atom in order to avoid interference between two CO-releasing steps as obviously detected for CORM-S2. In addition, an NMR probe should be introduced enabling the observation not only of CO release but also of the degradation of the metal complex. This procedure allows direct comparison of the analytical methodologies and at best validation of the myoglobin assay for photo-CORMs. Therefore, we investigated complexes of the type $[Fe(CO)(NC\text{-}Me)(H_2NCH_2CH_2PPh_2)_2]^{2+}$ (CORM-P1) and $[Fe(CO)(NC\text{-}Me)(H_2NC_6H_4\text{-}2\text{-}PPh_2)_2]^{2+}$ (CORM-P2), the counter anions being tetrafluoroborate, with the ^{31}P nucleus being a very sensitive NMR probe.

1. Results and discussion

1.1. Synthesis

The reactions of $[Fe(H_2O)_6]$ $[BF_4]_2$ with aminoethyl-diphenylphosphane and 2-(diphenylphosphino)aniline in acetonitrile solvent yielded the complexes *trans*-$[Fe(NC\text{-}Me)_2(H_2NCH_2CH_2PPh_2)_2]$ $[BF_4]_2$ (**1a**) [44] and *trans*-$[Fe(NC\text{-}Me)_2(H_2NC_6H_4\text{-}2\text{-}PPh_2)_2]$ $[BF_4]_2$ (**1b**). Exposing these complexes, dissolved in CH_2Cl_2, to a CO atmosphere led to substitution of one acetonitrile molecule by a carbon monoxide ligand under maintenance of the residual iron(II) environment, yielding $[Fe(CO)(NC\text{-}Me)(H_2NCH_2CH_2PPh_2)_2]$ $[BF_4]_2$ (**2a**, CORM-P1) and $[Fe(CO)(NC\text{-}Me)(H_2NC_6H_4\text{-}2\text{-}PPh_2)_2]$ $[BF_4]_2$ (**2b**, CORM-P2) according to Scheme 1. Substitution of the second acetonitrile did neither occur at longer reaction periods nor at higher carbon monoxide pressure or higher temperature. Therefore, very pure iron(II) complexes were easily obtained and isolated with high yields. Iron(II) complexes with two or three carbon monoxide ligands usually show *cis* or facial arrangements of these molecules due to the strong *trans*-influence of carbon monoxide. Exceptions are described in mixed cyano/carbonyl iron(II) complexes [34] which can be explained by the isoelectronic nature of CO and CN^-.

In solution solvent-separated ions are observed. The NMR parameters of the tetrafluoroborate anion of **1a** and **1b** are very similar and do not depend on the cation, even though in the crystalline state N–H···F bridges are observed.

1.2. IR investigations

The symmetric and asymmetric stretching frequencies of the carbon monoxide ligands of CORM-S1 (2014, 1945 cm^{-1} [31]) and CORM-S2 (2035, 1976 cm^{-1} [32]) are observed at significantly lower wavenumbers than those of free carbon monoxide (2134 cm^{-1} [45]). The iron(II) complexes CORM-P1 (C≡N: 2303, C≡O: 1985 cm^{-1}) and CORM-P2 (C≡N: 2290, C≡O: 2001 cm^{-1}) also show two bands, in this case due to acetonitrile (free gaseous acetonitrile 2268 cm^{-1}) and carbon monoxide stretching vibrations. A shift of the C≡N stretching mode to higher wavenumbers upon coordination to Lewis acids represents a very common observation for such complexes [45,46] with acetonitrile acting as a π-donor [47]. The wavenumbers of the C≡N stretching modes of the CORMs **2a** and **2b** are significantly larger than observed for the *bis*(acetonitrile) iron(II) complexes **1a** (2163 cm^{-1}) and **1b** (2207 cm^{-1}) because CO is a strong π-acceptor supporting the π-donor ability of acetonitrile.

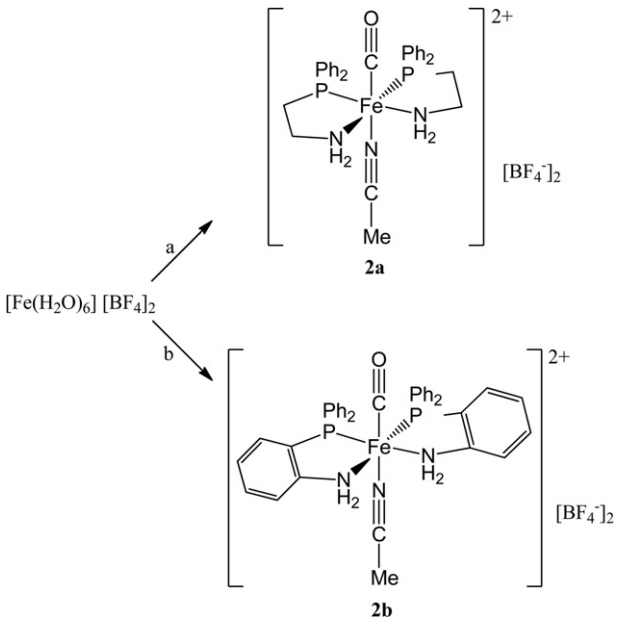

Scheme 1. Synthesis of the CO-releasing molecules **2a** (CORM-P1) and **2b** (CORM-P2), starting from $[Fe(H_2O)_6]$ $[BF_4]_2$. Reaction conditions: a) 1. Reaction with aminoethyl-diphenylphosphane in acetonitrile, 2. Substitution of one acetonitrile by CO; b) 1. Reaction with 2-diphenylphosphinoaniline in acetonitrile, 2. Substitution of one acetonitrile by CO.

1.3. Molecular structures

The cations *trans*-$[Fe(NC\text{-}Me)_2(H_2NCH_2CH_2PPh_2)_2]^{2+}$ [44] (counterion $[FeBr_4]^{2-}$) and *trans*-$[Fe(NC\text{-}Me)_2(H_2NC_6H_4\text{-}2\text{-}PPh_2)_2]^{2+}$ (**1b**) (Fig. 1, counterions $[BF_4]^-$ not displayed for clarity reasons) show very similar symmetries which deviate only slightly from C_{2v} symmetry. The iron(II) centers are in distorted octahedral environments with the acetonitrile ligands *trans* to each other. The diphenylphosphanyl groups are *cis*-arranged as are the amino groups.

The difference between these cations is the more rigid benzo-backbone of the cation of **1b** leading to smaller bites of the bidentate ligands and, hence, to slightly smaller P1–Fe1–N1 and P2–Fe1–N2 bond angles. The structural changes, however, are insignificant and even the P1–Fe1–P2 and N1–Fe1–N2 bond angles are very much alike. The nearly linear acetonitrile molecules show very short C≡N bond lengths. Whereas the more flexible ethylene backbone of *trans*-$[Fe(NC\text{-}Me)_2(H_2NCH_2CH_2PPh_2)_2]^{2+}$ allows to align to steric necessities, the more rigid benzo unit of **1b** suffers more severe distortions. Thus, the P1–C1–C2/6 and P2–C19–C20/24 angles differ by approximately 10° due to the bulky phenyl substituents at P1 and P2. For the small amino groups N1 and N2 the difference between proximal and distal N1–C6–C1/5 and N2–C24–C19/23 angles is much smaller.

Substitution of one acetonitrile ligand by a carbon monoxide reduces the symmetry of the cation and only the mirror plane containing the CO and NC–Me ligands is maintained. Fig. 2 shows $[Fe(CO)(NC\text{-}Me)(H_2NCH_2CH_2PPh_2)_2]$ $[BF_4]_2$ (**2a**, CORM-P1) and Fig. 3 displays the molecular structure of $[Fe(CO)(NC\text{-}Me)(H_2NC_6H_4\text{-}2\text{-}PPh_2)_2]$ $[BF_4]_2$ (**2b**, CORM-P2) clarifying also the stabilization by N–H···F hydrogen bridges to the tetrafluoroborate anions.

The structural parameters are very similar with respect to the carbonyl fragment. The CO bond lengths and the Fe–C distances with average values of 114.4 and 176.7 pm, respectively, differ only

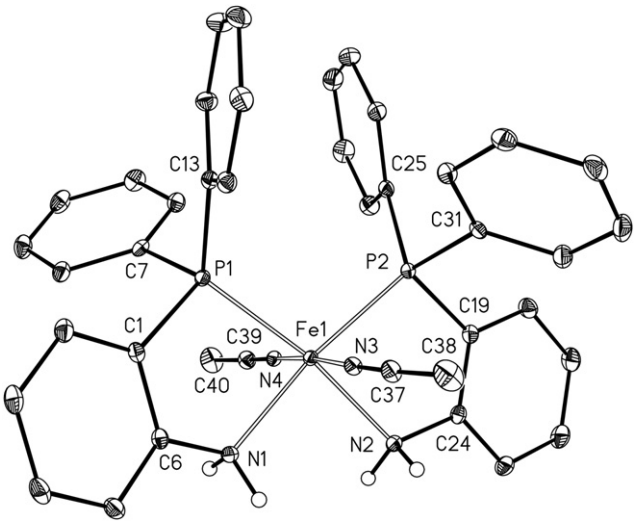

Fig. 1. Molecular structure and numbering scheme of the cation *trans*-[Fe(NC-Me)$_2$($H_2NC_6H_4$-2-PPh_2)$_2$]$^{2+}$ of **1b**. The ellipsoids represent a probability of 40%. H atoms with the exception of the amino groups are neglected for clarity reasons. Selected bond lengths (pm): Fe1–P1 223.72(5), Fe1–P2 222.66(5), Fe1–N1 206.0(2), Fe1–N2 205.8(2), Fe1–N3 192.0(2), Fe1–N4 191.5(2), N1–C6 145.2(2), N2–C24 145.7(2), N3–C37 114.1(2), N4–C39 114.0(2), P1–C1 182.1(2), P1–C7 182.8(2), P1–C13 182.4(2), P2–C19 181.3(2), P2–C25 182.0(2), P2–C31 183.1(2); angles (deg.): N3–Fe1–N4 175.99(6), P1–Fe1–P2 104.62(2), N1–Fe1–N2 88.14(6), P1–Fe1–N1 83.25(4), P2–Fe1–N2 84.05(4).

within their estimated standard deviations. Also the Fe–C–O angles of 178.6° for both cations deviate only insignificantly from linearity. The acetonitrile ligand experiences a significant Fe–N bond elongation due to the trans-positioned CO molecule by approximately 4 pm as a consequence of a weakened π-backdonation of electron density from the metal center to the π^* orbitals of the nitrile group. This fact is in agreement with the IR spectroscopic findings. The effect on the C≡N bond lengths is much smaller and lies within the standard deviations. However, the presence of the CO ligand also leads to elongation of the Fe–P bonds by approximately 2–3 pm.

The tetrafluoroborate anions form hydrogen bridges to the amino groups of the cations. In the compounds **1b** and **2b** (CORM-P2) the benzo-backbone fixes the nearly parallel alignment of the NH bonds of the amino groups. The BF_4^--anions are able to form two intramolecular N–H···F bridges to the same cation. Contrary to this formation of a contact ion pair due to the flexibility of the ethylene backbone in CORM-P1 (**2a**), the tetrafluoroborate anions form N–H···F bridges to two different cations leading to the formation of a dimeric contact ion pair.

1.4. CO release of CORM-P1 and CORM-P2

To infer about the mechanism of CO release we studied the light-triggered degradation of the CORMs by ^{31}P NMR spectroscopy. For this purpose CORM-P1 **2a** and CORM-P2 **2b** were dissolved in [D_6] dimethylsulfoxide (DMSO) at a final concentration of 23 mM. As expected, both CORMs showed no degradation in the dark. In order to quantitatively record the degradation of CORM-P1, the phosphorus-containing reference compound tetraphenylphosphonium chloride [Ph_4P Cl: $\delta(^{31}P) = 23.2$] was added. From this solution the degradation was observed in dependency of the irradiation duration (Fig. 4). The free ligand aminoethyl-diphenylphosphane was formed during CO release, and no other intermediates were detected by $^{31}P\{^1H\}$ NMR spectroscopy.

A different picture resulted from a [D_3]acetonitrile solution of CORM-P1, again at 23 mM. Already in the dark a very slow

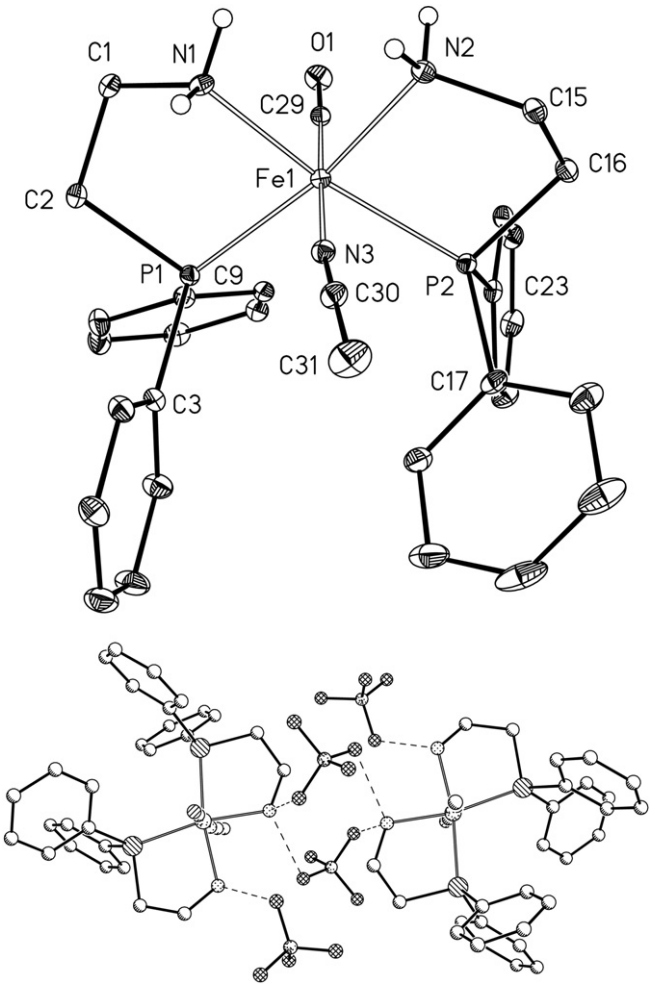

Fig. 2. Molecular structure and numbering scheme of the cation [Fe(CO)(NC-Me)($H_2NCH_2CH_2PPh_2$)$_2$]$^{2+}$ (**2a**, CORM-P1) (top). The ellipsoids represent a probability of 40%, all C-bound H atoms are omitted for clarity reasons. At the bottom, dimer formation via a N–H···F network of [Fe(CO)(NC-Me)($H_2NCH_2CH_2PPh_2$)$_2$] [BF_4]$_2$ is represented. Here arbitrary radii were chosen for all atoms. Selected bond lengths (pm): Fe1–P1 228.84(5), Fe1–P2 228.55(5), Fe1–N1 204.4(2), Fe1–N2 205.9(2), Fe1–N3 194.7(2), Fe1–C29 176.4(2), C29–O1 114.4(2), N1–C1 148.5(2), N2–C15 149.0(2), N3–C30 114.1(3), P1–C2 185.0(2), P1–C31 83.4(2), P1–C9 182.5(2), P2–C16 183.3(2), P2–C17 181.5(2), P2–C23 182.3(2); angles (deg.): N3–Fe1–C29 178.11(8), P1–Fe1–P2 106.85(2), N1–Fe1–N2 86.00(7), P1–Fe1–N1 83.32(5), P2–Fe1–N2 83.68(5), Fe1–C29–O1 178.5(2).

decomposition was observed leading to a quantitative conversion to *trans*-[Fe(NC-Me)$_2$($H_2NCH_2CH_2PPh_2$)$_2$] [BF_4]$_2$ (**1a**) and carbon monoxide within two weeks. Irradiation of a freshly prepared solution of **2a** in D_3C–C≡N led to CO liberation and formation of **1a**. Therefore, initially no free ligand was observed. However, *trans*-[Fe(NC-Me)$_2$($H_2NCH_2CH_2PPh_2$)$_2$] [BF_4]$_2$ (**1a**) also degrades during irradiation but this breakup is slower than the decomposition of CORM-P1 (**2a**). The $^{31}P\{^1H\}$ NMR spectra of this degradation reaction are shown in Fig. 5, the interpretation is displayed in Fig. 6. Here it becomes obvious that there is an induction period for the appearance of $H_2NCH_2CH_2PPh_2$ due to the intermediate formation of **1a**. A control experiment verified that a solution of *trans*-[Fe(NC-Me)$_2$($H_2NCH_2CH_2PPh_2$)$_2$] [BF_4]$_2$ (**1a**) in [D_3]acetonitrile is stable in the dark but that this complex degrades upon irradiation liberating free aminoethyl-diphenylphosphane.

We further assayed the properties of the compounds in aqueous solutions. CO release was quantified in a myoglobin-based assay by spectrophotometric measurement of the conversion of

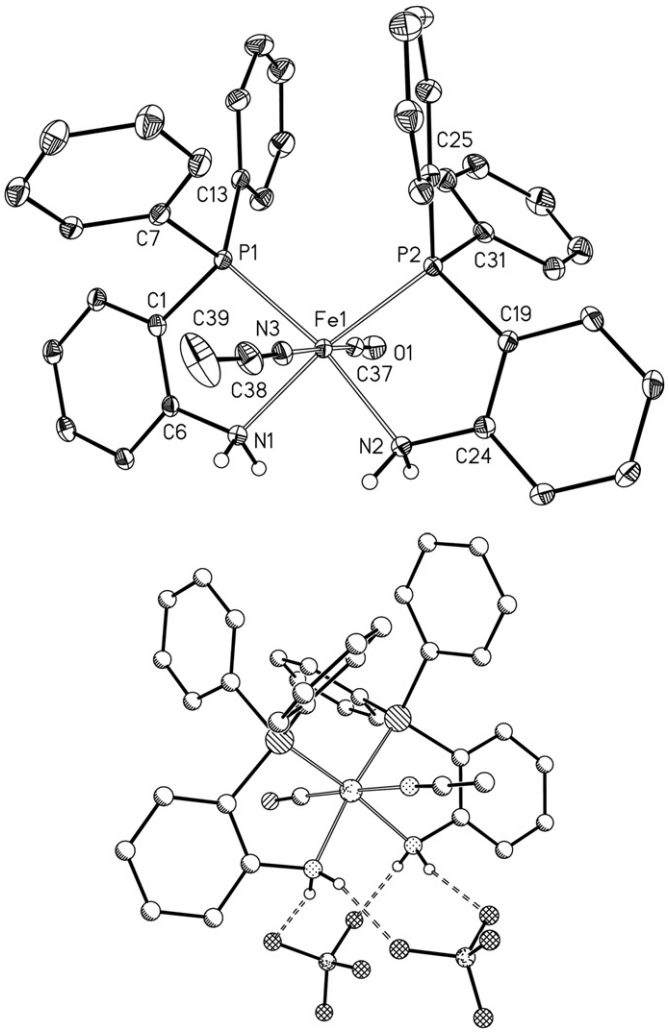

Fig. 3. Molecular structure and numbering scheme of the cation $[Fe(CO)(NC\text{-}Me)(H_2NC_6H_4\text{-}2\text{-}PPh_2)_2]^{2+}$ of **2b** (CORM-P2) (top). The ellipsoids represent a probability of 40%. All C-bound hydrogen atoms are neglected for clarity reasons. At the bottom, the structure of $[Fe(CO)(NC\text{-}Me)(H_2NC_6H_4\text{-}2\text{-}PPh_2)_2]\ [BF_4]_2$ (**2b**, CORM-P2) is shown, displaying the formation of a contact ion pair via N–H···F bridges. The atoms are drawn with arbitrary radii. Selected bond lengths (pm): Fe1–P1 225.50(8), Fe1–P2 225.32(8), Fe1–N1 206.3(2), Fe1–N2 206.0(2), Fe1–N3 195.6(2), Fe1–C37 176.9(3), C37–O1 114.3(4), N1–C6 145.9(4), N2–C24 146.0(4), N3–C38 113.5(4), P1–C1 181.2(3), P1–C7 181.9(3), P1–C13 181.8(3), P2–C19 181.2(3), P2–C25 182.0(3), P2–C31 182.6(3); angles (deg.): N3–Fe1–C37 178.4(1), P1–Fe1–P2 103.79(3), N1–Fe1–N2 87.1(1), P1–Fe1–N1 84.32(7), P2–Fe1–N2 84.91(7), Fe1–C37–O1 178.6(3).

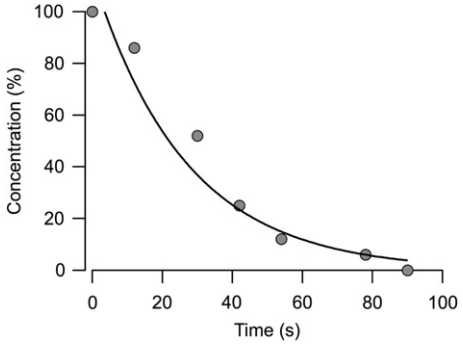

Fig. 4. Time-dependent degradation of **2a** (CORM-P1) upon irradiation with visible light in a 23-mM solution of **2a** in $[D_6]$DMSO followed by $^{31}P\{^1H\}$ NMR spectroscopy. For quantification reasons Ph_4P Cl was added as a reference compound. The continuous curve is the result of a single-exponential data fit with a time constant of 21 s.

deoxymyoglobin (Mb) into the myoglobin–CO complex (Mb–CO). For measurements in the range of 500–600 nm a solution was prepared that contained equimolar (100 μM) amounts of deoxymyoglobin and either CORM-P1 or CORM-P2. Myoglobin was reduced with 0.1% sodium dithionite. Both CORMs showed no CO release in the dark but irradiation with white light for 10 min led to quantitative (Fig. 7A, left, CORM-P1) or incomplete (Fig. 7A, right, CORM-P2) carbon monoxide liberation. However, monitoring of the CO release of CORM-P2 in this wavelength range, which requires a high concentration, was less accurate because of the self-absorbance of this complex. We therefore also investigated the light-dependent CO release at lower concentration (5 μM) in a spectral range covering the Soret peak (Fig. 7B). The CORMs were irradiated for 10 min in a buffered solution, which contained 0.1% of sodium dithionite and a concentration of 10 μM deoxymyoglobin, and the spectra without and with irradiated CORMs were compared (Fig. 7B for irradiation with 420-nm light). While stable in the dark, light completely released CO from CORM-P1. For the benzo derivative CORM-P2, however, the release was incomplete. A comparable observation was also valid for a comparison of $[(OC)_2Fe(SCH_2CH_2NH_2)_2]$ (CORM-S1) and $[(OC)_2Fe(SC_6H_4NH_2)_2]$ (CORM-S2) [32].

Kinetics of CO release was monitored by measuring the change in absorbance at 422 nm. When exposing the samples to light of 420, 470, or 520 nm, CO release followed a single-exponential time course (Fig. 7C). The corresponding time constants strongly increased with the wavelength (Fig. 7D). For CORM-P1, total release of the CO could be obtained for all wavelengths in the chosen experimental setting, while for CORM-P2 only a partial release was observed (Fig. 7E).

As it was reported for CORM-2 and CORM-3 that CO release is strongly facilitated by the reducing agent dithionite [43], we also performed experiments in which CO release was triggered by light in the absence of dithionite. Such experiments (Fig. 8) clearly showed that dithionite itself does not release CO from the compounds studied, which is in agreement with the NMR experiments shown above.

2. Conclusion

Substitution of one acetonitrile ligand in *trans*-$[Fe(NC\text{-}Me)_2(H_2NCH_2CH_2PPh_2)_2]\ [BF_4]_2$ (**1a**) and *trans*-$[Fe(NC\text{-}Me)_2(H_2NC_6H_4\text{-}2\text{-}PPh_2)_2]\ [BF_4]_2$ (**1b**) succeeds quantitatively in a carbon monoxide atmosphere yielding $[Fe(CO)(NC\text{-}Me)(H_2NCH_2CH_2PPh_2)_2]\ [BF_4]_2$ (**2a**, CORM-P1) and $[Fe(CO)(NC\text{-}Me)(H_2NC_6H_4\text{-}2\text{-}PPh_2)_2]\ [BF_4]_2$ (**2b**, CORM-P2), respectively, with a *trans*-arrangement of the CO and the acetonitrile ligands. Both CORMs **2a** and **2b** readily lose the carbon monoxide ligand upon irradiation with visible light making these complexes valuable photo-CORMs.

Irradiation of **2a** leads to loss of CO followed by complex degradation and formation of free aminoethyl-diphenylphosphane. A $^{31}P\{^1H\}$ NMR study in $[D_6]$DMSO revealed that the iron(II) complex **2a** degrades completely after light-induced loss of CO also simultaneously liberating aminoethyl-diphenylphosphane. If $[D_3]$ acetonitrile is chosen as solvent for this experiment another degradation pathway is observed. In this solvent, loss of carbon monoxide upon irradiation with visible light yields *trans*-$[Fe(NC\text{-}Me)_2(H_2NCH_2CH_2PPh_2)_2]\ [BF_4]_2$ (**1a**). This *bis*(acetonitrile) iron(II) complex **1a** also degrades upon irradiation but this decomposition is much slower than the CO release from **2a**. Therefore, the following mechanism can be formulated for the decomposition of **2a** in visible light: upon irradiation of **2a**, CO is substituted by another acetonitrile ligand yielding **1a**. This complex also degrades in visible light finally forming uncoordinated aminoethyl-diphenylphosphane. However, this second degradation step is significantly slower than the light-induced CO release step.

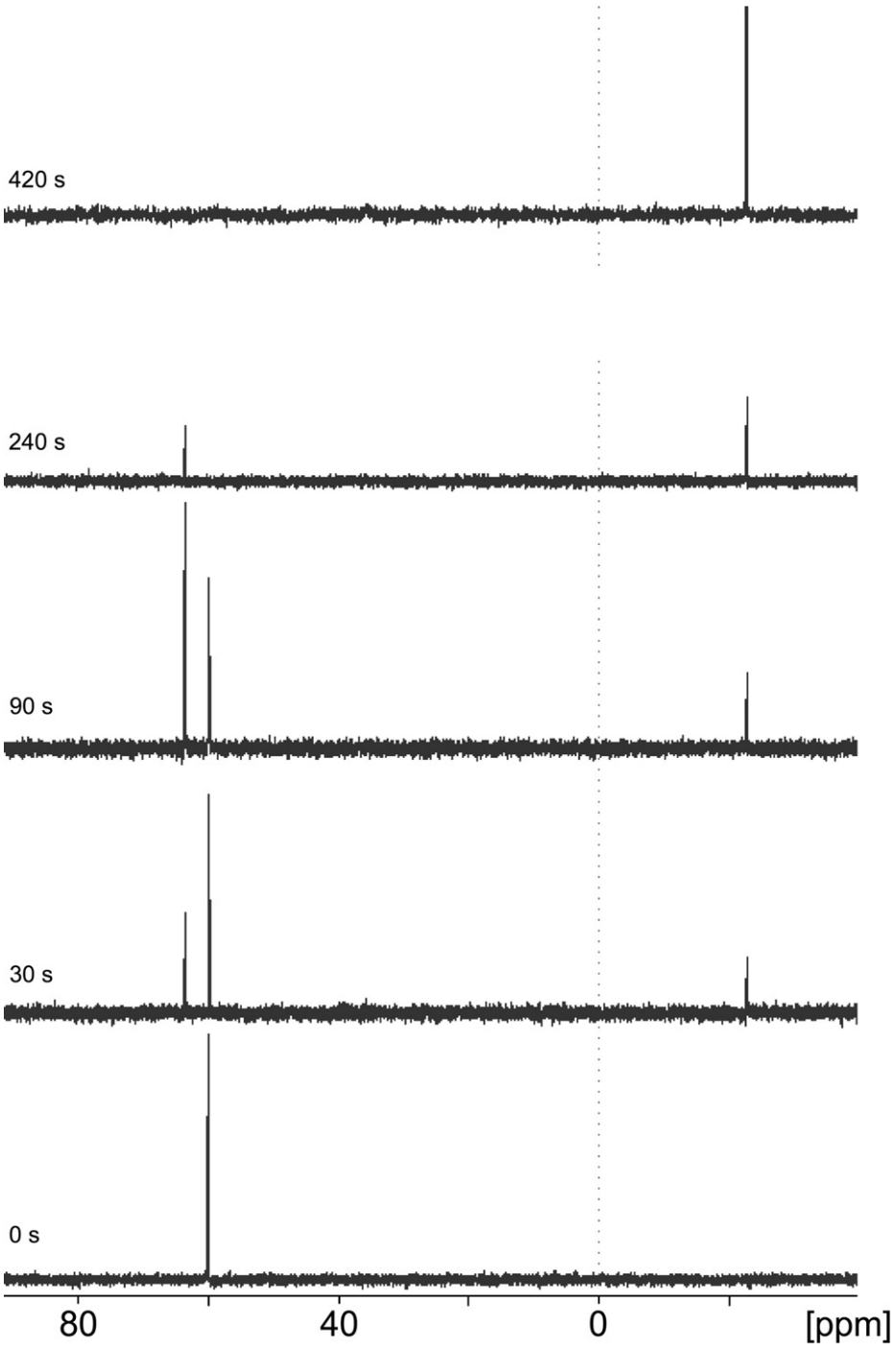

Fig. 5. $^{31}P\{^{1}H\}$ NMR spectra of the degradation of a 23-mM solution of CORM-P1 (**2a**) in [D_3]acetonitrile during irradiation with visible light. The bottom spectrum shows the resonance of pure CORM-P1 ($t = 0$ s, $\delta = 61.7$). The spectra were recorded at the indicated times. During irradiation with light of 470 nm, the signals of *trans*-[$Fe(NC\text{-}Me)_2(H_2NCH_2CH_2PPh_2)_2$] [$BF_4$]$_2$ (**1a**) ($\delta = 63.7$) and free aminoethyl-diphenylphosphane ($\delta = -21.0$) appear. The resonance of starting **2a** disappears and finally, also the acetonitrile complex **1a** vanishes. Only the signal of free aminoethyl-diphenylphosphane can be recognized after 420 s (top spectrum).

Substitution of the ethylene backbone by a benzo unit giving **2b** alters the CO release properties significantly. Iron(II) complex **2b** also liberates carbon monoxide upon irradiation with visible light but the CO liberation is much slower than observed for **2a** and incomplete. This observation is in agreement with earlier studies of [$(OC)_2Fe(SCH_2CH_2NH_2)_2$] (CORM-S1) and [$(OC)_2Fe(SC_6H_4\text{-}2\text{-}NH_2)_2$] (CORM-S2); in these thiolate iron(II) complexes the benzo-backbone also diminishes the beneficial light-induced CO release properties.

The myoglobin–CO assay is a useful tool in order to follow the degradation of photo-CORMs. Despite the fact that McLean et al. [43] concluded that "the classification of CORMs on the basis of the Mb–CO assay must be abandoned", this statement is mainly based on CORMs with a ligand exchange triggering the CO release. Here we could verify (Fig. 8) that for these photo-CORMs this simple and fast Mb–CO assay still represents a valuable method to determine the CO liberation. For the determination of CO release from colored metal carbonyls it is advantageous to choose a detection wavelength of 422 nm.

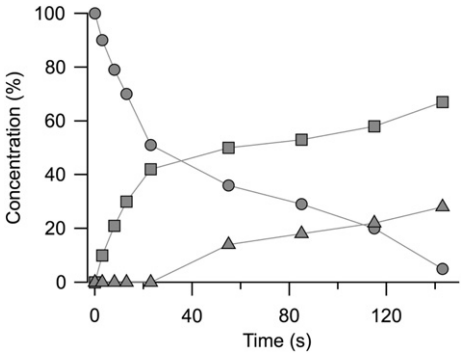

Fig. 6. Light-induced degradation of **2a** (circles, CORM-P1) in a 23-mM [D_3]acetonitrile solution. During the first 20 s, CO is substituted by acetonitrile yielding *trans*-[Fe(NC-Me)$_2$($H_2NCH_2CH_2PPh_2$)$_2$] [BF_4]$_2$ (**1a**, squares). Thereafter, the resonance of free aminoethyl-diphenylphosphane (triangles) is detected originating from light-triggered decomposition of complex **1a**. Competing formation of **1a** from ligand substitution in **2a** and light-induced decomposition of **1a** implicate a rather constant concentration of **1a** after approximately 60 min. Straight lines connect data points for clarity.

3. Experimental

3.1. Materials and methods

CO release was measured spectrophotometrically based on absorbance changes upon conversion of deoxymyoglobin (Mb) to the myoglobin–CO complex (Mb–CO). Horse skeletal muscle myoglobin (Sigma) in phosphate buffered saline (PBS) was reduced to deoxymyoglobin by addition of 0.1% sodium dithionite. Difference spectra for 100 μM Mb with and without CORMs were initially measured in the range of 500–600 nm (Fig. 7A). However, because of the strong self-absorbance of CORM-P2 further experiments were performed at lower concentration (5 μM CORM and 10 μM Mb) in a spectral range covering the Soret region (380–450 nm). Spectra in the absence of CO and in CO-saturated solution were recorded to calculate the maximal absorbance difference, required to convert absorbance changes to relative CO release. The time course of CO release from CORMs was monitored by measuring absorbance at 422 nm every 10 s. For illumination we used a cold light source (20 W halogen lamp, Osram GZX4) with a light guide yielding 2 W output power placed 2 cm above the cuvette. In addition, a monochromator based on a 150-W xenon lamp (Polychrome V, TILL Photonics, Gräfelfing, Munich, Germany) was used to generate light of 15 nm bandwidth (at 50% of the intensity) to stimulate CORM breakdown with a defined wavelength. At the end of the light guide placed directly above the cuvette output powers of 12.9 mW at 420 nm, 15.2 mW at 470 nm, and 11.3 mW at 520 nm were obtained. To test for dependence of CO release from light, myoglobin, or dithionite, samples were preincubated for 10 min under different conditions. Spectra in the Soret region were recorded immediately after addition of myoglobin and sodium dithionite at their final concentrations of 10 μM and 0.1%, respectively.

3.2. Synthesis of trans-[Fe(NC-Me)$_2$($H_2NCH_2CH_2PPh_2$)$_2$] [BF_4]$_2$ (**1a**)

This complex was prepared according to a literature procedure [44]. To a stirring solution of [Fe(H_2O)$_6$][BF_4]$_2$ (100 mg, 0.296 mmol) and CH_3CN (5 ml) was added 2-(diphenylphosphino)ethylamine (136 mg, 0.593 mmol) in CH_3CN (1 ml) dropwise. The mixture turned purple immediately and was stirred for 30 min. Then the solvent was removed in vacuo and the residue was dissolved in 1 ml of CH_2Cl_2. The addition of 10 ml of diethyl ether yielded a purple solid, which was isolated by filtration and dried in vacuum (212 mg, 0.275 mmol, 93%). ^{11}B NMR (128.38 MHz, [D_6]DMSO): δ −1.3. ^{19}F NMR (188.31 MHz, [D_6]DMSO): δ −151.9. ^{31}P{^{1}H} NMR (161.95 MHz, CD_3CN): δ 63.7. IR: 3330 (w); 2163 (s); 1604(s); 1312 (w); 873 (vs); 695 (w); 646(s); 607 (vs); 511(w); 495 (m); 480 (m).

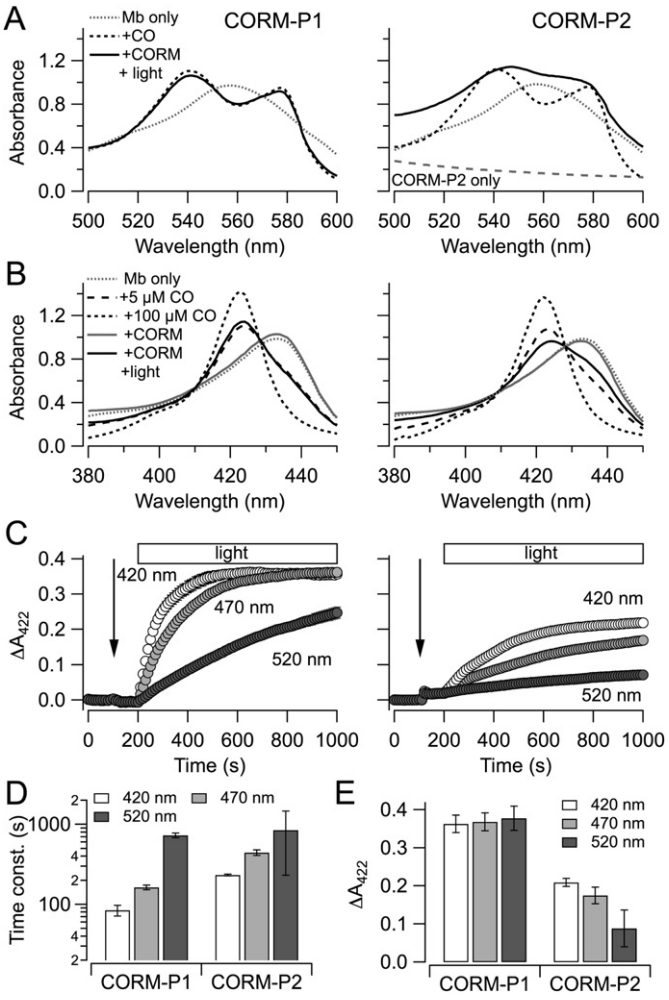

Fig. 7. Light-dependent CO release. (A) Absorption spectra for 100 μM CORM-P1 (left) and CORM-P2 (right) irradiated with white light for 10 min in PBS + 0.1% sodium dithionite + 100 μM deoxymyoglobin (Mb) (black line). Absorption spectra for CO-free (dotted line) and CO-saturated (dashed line) Mb are shown for comparison. Also indicated is the self-absorbance of CORM-P2, which precludes the use of this assay for quantitative CO release determination. (B) Absorption spectra in the range of 380–450 nm for 5 μM of the indicated CORMs and 10 μM deoxymyoglobin upon 10-min irradiation with 420-nm light. For controls Mb with 5 μM (long dashes) and 100 μM CO (short dashes), as well as Mb with CORMs before irradiation (grey line) are shown. (C) Absorbance changes at 422 nm (ΔA_{422}) as a function of time for the indicated wavelengths. The arrows indicate addition of 5 μM CORM-P1 (left) or CORM-P2 (right). Samples were illuminated 100 s later, as indicated by the horizontal bar. The instantaneous increase in absorbance upon addition of CORM-P2 originates from the absorbance of the CORM. (D, E) The time courses in (C) were fit with single-exponential functions and the resulting time constants (D) and the maximal absorbance changes (E) are shown for the indicated wavelengths. The bars labeled "CO" show the absorbance change obtained when adding 10 μM Mb to a solution containing 5 μM CO, i.e. they mark the maximal possible release of CO from the CORMs studied. All data shown are means ± sem for n = 4–5.

3.3. Synthesis of [Fe(CO)(NC-Me)($H_2NCH_2CH_2PPh_2$)$_2$] [BF_4]$_2$ (**2a**, CORM-P1)

For the synthesis of **2a** the isolation of complex **1a** is not required. Therefore, aminoethyl-diphenylphosphane (136 mg, 0.593 mmol) was added dropwise to a stirred solution of [Fe(H_2O)$_6$]

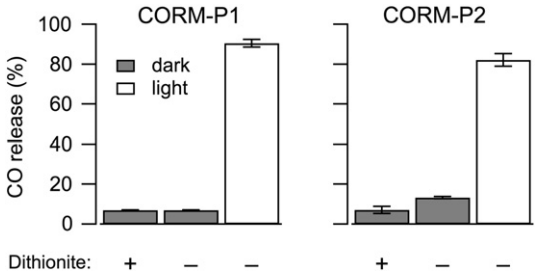

Fig. 8. CO release is not dependent on dithionite. CO release by CORM-P1 and CORM-P2 during 10-min preincubation without Mb in the presence ("+") or absence ("–") of dithionite, with (open bars) or without (grey bars) illumination with white light. Spectra were taken right after preincubation and subsequent mixing of the samples with Mb/dithionite. Experimental conditions as in Fig. 7A. Data are means ± sem for $n = 4–5$.

$[BF_4]_2$ (100 mg, 0.296 mmol) in 5 ml of CH_3CN yielding a purple reaction mixture. After removal of all volatiles in vacuo and dissolution of the residue with 10 ml of CH_2Cl_2, this solution was treated with gaseous CO for 16 h. During this time a yellow suspension formed. CORM-P1 was isolated as a yellow solid (190 mg, 0.251 mmol, 91%) by filtration and the filter cake dried in vacuum. Recrystallization of a small portion of this powder from a mixture of CH_2Cl_2 and DMF/Et_2O by using the slow diffusion method yielded dark orange single crystals suitable for X-ray diffraction experiments. Physical data: M.p.: 202–205 °C. NMR: ^{1}H NMR (600.13 MHz, [D_6]DMSO): δ 2.18 (s, 3H), 2.92 (broad, 4H), 4.07 (broad, 4H), 4.8 (broad, 4H), 7.04 (d, 8H), 7.36 (*t*, 8H), 7.57 (*t*, 4H). ^{11}B NMR (128.38 MHz, [D_6]DMSO): δ −1.3. ^{13}C{^{1}H} NMR (150.90 MHz, [D_6]DMSO): δ: 4.22 (broad), 31.02 (m), 41.46 (broad), 129.22 (d), 131.47 (d), 132.11 (d), 133.30 (broad), 160.63 (broad), 215.20 (broad). ^{19}F NMR (188.31 MHz, [D_6]DMSO): δ −148.7. ^{31}P{^{1}H} NMR (161.95 MHz, [D_6]DMSO): δ 61.7 (s). MS-ESI: 257 $[Fe(Ph_2PC_2H_4NH_2)_2]^{2+}$ (100); 229 $[(Ph_2PC_2H_4NH_2)_2]^{2+}$ (16); 185 $[(Ph_2P)_2]^{2+}$ (37). IR [Nujol, KBr windows]: 3555 (w); 3307(s); 3269 (s); 3175(m); 3065 (m); 2922 (vs); 2854 (vs); 2303 (m); 1985(vs); 1597 (m); 1460 (s); 1436 (s); 1376(m); 1256 (m); 1094(vs); 1042 (vs); 1011 (s); 996 (s); 929 (w); 816 (w); 747 (s); 697 (s); 594 (m); 529 (s); 510 (m); 475 (w). Elemental analysis ($C_{31}H_{35}B_2F_8FeN_3OP_2$, 757.03 g mol^{-1}): calc.: C 49.18; H 4.66; N 5.55; found: C 48.93; H 4.35; N 5.35.

3.4. Synthesis of trans-[Fe(NC-Me)$_2$($H_2NC_6H_4$-2-PPh_2)$_2$] $[BF_4]_2$ (**1b**)

For the synthesis of *trans*-[Fe(NC-Me)$_2$($H_2NC_6H_4$-2-PPh_2)$_2$] $[BF_4]_2$ (**1b**) 2-(diphenylphosphino)aniline (164 mg, 0.593 mmol) in CH_3CN (1 ml), which was prepared as described previously [48], was added dropwise to a stirred solution of $[Fe(H_2O)_6][BF_4]_2$ (100 mg, 0.296 mmol) in CH_3CN (5 ml). The reaction mixture turned purple immediately and was stirred for an additional hour. Thereafter, the solvent was removed in vacuo and the residue dissolved in 1 ml of CH_2Cl_2. The addition of 10 ml of diethyl ether afforded a purple solid, which was isolated by filtration and dried in vacuum (241 mg, 0.278 mmol, 94%). Recrystallization of a small portion of this solid from CH_3CN/Et_2O by using the slow diffusion method gave violet single crystals suitable for X-ray diffraction experiments. Physical data: M.p.: 211–213 °C. NMR: ^{1}H NMR (400.08 MHz, CD_3CN): δ 1.96 (s, 6H), 5.94 (s, 4H), 6.87 (*t*, 8H), 7.33 (*t*, 8H), 7.53 (*t*, 8H), 7.73 (m, 2H), 7.84 (d, 2H). ^{13}C{^{1}H} NMR (150.90 MHz, CD_3CN): δ 3.85 (t), 128.00 (t), 128.77 (t), 129.96 (t), 130.85 (m), 131.67 (s), 132.96 (m), 133.36 (t), 133.66 (s), 134.85 (s), 137.95(s), 151.37 (t). ^{31}P{^{1}H} NMR (161.95 MHz, CD_3CN): δ 68.1 (s). MS-ESI: 305 $[Fe(PPh_2C_6H_4\text{-}2\text{-}NH_2)_2]^{2+}$ (100); 277 $[(PPh_2C_6H_4\text{-}2\text{-}NH_2)_2]^{2+}$ (90). IR: 3280 (s); 2207(s); 1607(w); 1566 (m); 1478 (s); 1436 (s); 1094 (vs); 1047 (vs); 820 (w); 756 (s); 694 (s); 575 (m); 520 (vs); 485 (m); 471 (vs); 458 (s); 415 (m); 929 (w); 816 (w); 747 (s); 697 (s); 594 (m); 529 (s); 510 (m); 475 (w). Elemental analysis ($C_{44}H_{44}B_2F_8FeN_6P_2$, 948.26 g mol^{-1}): calc.: C 55.73; H 4.68; N 8.86; found: C 55.62; H 4.68; N 8.76.

3.5. Synthesis of [Fe(CO)(NC-Me)($H_2NC_6H_4$-2-PPh_2)$_2$] $[BF_4]_2$ (**2b**, CORM-P2)

For the synthesis of CORM-P2, **1b** (241 mg, 0.278 mmol) was dissolved in 10 ml of CH_2Cl_2 and stirred under a CO atmosphere for 16 h. The resulting orange–yellow solution was evaporated to dryness to leave a yellow powder, which was washed with diethyl

Table 1
Crystal data and refinement details for the X-ray structure determinations of the compounds **1**–**2b**.

Compound	**1b**	**2a**	**2b**
Formula	$[C_{40}H_{38}FeN_4P_2]^{2+}$, 2$[BF_4]^-$, 2($C_2H_3N$)	$[C_{31}H_{35}FeN_3OP_2]^{2+}$, 2$[BF_4]^-$	$[C_{39}H_{35}FeN_3OP_2]^{2+}$, 2$[BF_4]^-$, CH_2Cl_2
fw (g mol^{-1})	948.26	757.03	938.04
T/°C	−140(2)	−140(2)	−140(2)
Crystal system	Triclinic	Triclinic	Monoclinic
Space group	$P\bar{1}$	$P\bar{1}$	$P2_1/n$
a/Å	11.3798(2)	9.8383(1)	13.4610(3)
b/Å	12.4188(2)	11.7972(3)	23.0816(4)
c/Å	17.8206(3)	14.4190(3)	13.5722(3)
α/°	74.966(1)	98.138(1)	90
β/°	85.178(1)	92.800(1)	100.427(1)
γ/°	68.964(1)	95.042(1)	90
V/Å^3	2270.05(7)	1647.08(6)	4147.26(15)
Z	2	2	4
ρ (g cm^{-3})	1.387	1.526	1.502
μ (cm^{-1})	4.75	6.32	6.43
Measured data	14,722	9907	23,878
Data with $I > 2\sigma(I)$	9507	6869	7781
Unique data (R_{int})	10,305/0.0197	7443/0.0151	9451/0.0390
wR_2 (all data, on F^2)[a]	0.0986	0.0828	0.1347
R_1 ($I > 2\sigma(I)$)[a]	0.0390	0.0380	0.0547
s[b]	1.057	1.070	1.054
Res. dens./e Å^{-3}	0.589/−0.469	0.822/−0.441	0.843/−0.979
CCDC No.	905061	905062	905063

[a] Definition of the R indices: $R_1 = (\sum||F_o| - |F_c||)/\sum|F_o|; wR_2 = \{\sum[w(F_o^2 - F_c^2)^2]/\sum[w(F_o^2)^2]\}^{1/2}$ with $w^{-1} = \sigma^2(F_o^2) + (aP)^2 + bP; P = [2F_c^2 + \mathrm{Max}(F_o^2)]/3$.
[b] $s = \{\sum[w(F_o^2 - F_c^2)^2]/(N_o - N_p)\}^{1/2}$.

ether. CORM-P2 was isolated as a yellow powder (218 mg, 0.256 mmol, 92%). Recrystallization of a small portion of this powder from a solvent mixture of CH_2Cl_2 and DMF/Et_2O using the slow diffusion method yielded light orange single crystals suitable for X-ray diffraction experiments. Physical data: M.p.: 216–218 °C. ^{1}H NMR (400.08 MHz, [D$_6$]DMSO): δ 2.04 (s, 3H, CH_3), 5.71 (s, 4H, H_2N), 6.92 (broad 8H), 7.39 (dd, 8H), 7.57 (broad, 8H), 7.76 (broad, 2H), 7.94 (broad, 2H). ^{13}C{^{1}H} NMR (100.60 MHz, [D$_6$]DMSO): δ 3.19 (s), 126.36 (m), 127.20 (m), 128.10 (t), 129.67 (s), 130.86 (d), 131.32 (m), 132.50 (d), 132.88 (d), 133.11 (m), 134.99 (d), 162.12 (broad), 206.35 (broad). ^{31}P{^{1}H} (161.95 MHz, CD_3CN): δ 58.2 (s). MS-ESI: 305 $[Fe(PPh_2C_6H_4\text{-}2\text{-}NH_2)_2]^{2+}$ (100); 277 $[(PPh_2C_6H_4\text{-}2\text{-}NH_2)_2]^{2+}$ (90); 201 $[(PPh_2\text{-}NH_2)_2]^{2+}$ (7). IR: 3280 (s); 2290 (m); 2001 (vs); 1590 (w); 1480(s); 1437 (s); 1096 (w); 1056 (vs); 751 (s); 696 (vs); 578 (m); 516 (vs); 464 (vs); 448 (m); 411 (w). Elemental analysis ($C_{40}H_{37}B_2Cl_2F_8FeN_3OP_2$, 938.04 g mol^{-1}): calc.: C 51.22; H 3.98; N 4.48; found: C 50.76; H 4.03; N 4.65.

3.6. Structure determinations

The intensity data for the compounds were collected on a Nonius KappaCCD diffractometer using graphite-monochromated Mo-K_α radiation. Data were corrected for Lorentz and polarization effects but not for absorption effects [49,50].

The structures were solved by direct methods (SHELXS [51]) and refined by full-matrix least squares techniques against F_o^2 (SHELXL-97 [51]). All hydrogen atoms for compound **1b**, the amine hydrogen atoms of **2a** and **2b** additional to the acetonitrile hydrogen atoms of **2a** were located by difference Fourier synthesis and refined isotropically [51]. All other hydrogen atoms were included at calculated positions with fixed thermal parameters. All non-hydrogen atoms were refined anisotropically [51]. Crystallographic data as well as structure solution and refinement details are summarized in Table 1. XP (SIEMENS Analytical X-ray Instruments, Inc.) was used for structure representations.

Acknowledgments

We thank Robert Braun for technical assistance, and the German Research Foundation (DFG, Bonn-Bad Godesberg/Germany) for generous financial support within the collaborative research group FOR 1738. T.M.A. Jazzazi is also grateful to the Carl Zeiss Foundation/Stuttgart (Germany) for a Ph.D. grant. Infrastructure of our institute was provided by the EU (European Fonds for Regional Development, EFRE) and the Friedrich Schiller University Jena.

Appendix A. Supporting Information available

Crystallographic data (excluding structure factors) has been deposited with the Cambridge Crystallographic Data Centre as supplementary publication CCDC-905061 for **1b**, CCDC-905062 for **2a**, and CCDC-905063 for **2b**. Copies of the data can be obtained free of charge on application to CCDC, 12 Union Road, Cambridge CB2 1EZ, UK [E-mail: deposit@ccdc.cam.ac.uk].

Appendix B. Supplementary data

Supplementary data related to this article can be found at http://dx.doi.org/10.1016/j.jorganchem.2013.02.015.

References

[1] B.E. Mann, Top. Organomet. Chem. 32 (2010) 247–285.
[2] A. Hermann, G.F. Sitdikova, T.M. Weiger, Biol. Unserer Zeit 40 (2010) 185–193.
[3] W.J. Wilkinson, P.J. Kemp, J. Physiol. 589 (2011) 3055–3062.
[4] C.C. Romão, W.A. Blättler, J.D. Seixas, G.J.L. Bernardes, Chem. Soc. Rev. 41 (2012) 3571–3583.
[5] R. Foresti, M.G. Bani-Hani, R. Motterlini, Intensive Care Med. 34 (2008) 649–658.
[6] R. Motterlini, L.E. Otterbein, Nat. Rev. Drug Discov. 9 (2010) 728–743.
[7] B.E. Mann, Organometallics 31 (2012) 5728–5735.
[8] B.E. Mann, T.R. Johnson, J.E. Clark, R. Foresti, C. Green, R. Motterlini, J. Inorg. Biochem. 96 (2003) 40.
[9] T.R. Johnson, B.E. Mann, J.E. Clark, R. Foresti, C.J. Green, R. Motterlini, Angew. Chem. Int. Ed. 115 (2003) 3850–3858; Angew. Chem. Int. Ed. 42 (2003) 3722–3729.
[10] D. Crespy, K. Landfester, U.S. Schubert, A. Schiller, Chem. Commun. 46 (2010) 6651–6662.
[11] U. Schatzschneider, Eur. J. Inorg. Chem. (2010) 1451–1467.
[12] U. Schatzschneider, Inorg. Chim. Acta 374 (2011) 19–23.
[13] R.D. Rimmer, A.E. Pierri, P.C. Ford, Coord. Chem. Rev. 256 (2012) 1509–1519.
[14] R. Alberto, R. Motterlini, Dalton Trans. (2007) 1651–1660.
[15] T.R. Johnson, B.E. Mann, I.P. Teasdale, H. Adams, R. Foresti, C.J. Green, R. Motterlini, Dalton Trans. (2007) 1500–1508.
[16] D.J. Kaczorowski, B.S. Zuckerbraun, Curr. Med. Chem. 14 (2007) 2720–2725.
[17] We are aware of a Fenton-type chemistry which might be one of the sources of reactive oxygen species (ROS) in biological systems because iron(II) ions react with oxygen yielding iron(III) species and O^{2-} ions with a subsequent characteristic chemistry. See e.g. (a) C. Walling, Acc. Chem. Res. 8 (1975) 125–131; (b) S. Goldstein, D. Meyerstein, G. Czapski, Free Radic. Biol. Med. 15 (1993) 435–445; (c) S. Liochev, I. Fridovich, Free Radic. Biol. Med. 16 (1994) 29–33.
[18] W. Cremer, Biochem. Z. 194 (1928) 231–232.
[19] W. Cremer, Biochem. Z. 206 (1929) 228–239.
[20] M.P. Schubert, J. Am. Chem. Soc. 55 (1933) 4563–4570.
[21] J.H. Wang, A. Nakahara, E.B. Fleischer, J. Am. Chem. Soc. 80 (1958) 1109–1113.
[22] A. Röder, E. Bayer, Angew. Chem. Int. Ed. 6 (1967) 263–264.
[23] A. Tomita, H. Hirai, S. Makishima, Inorg. Chem. 6 (1967) 1746–1749.
[24] A. Tomita, H. Hirai, S. Makishima, Inorg. Nucl. Chem. Lett. 4 (1968) 715–718.
[25] J. Takács, E. Soós, Z. Nagy-Magos, L. Markó, G. Gervasio, T. Hoffmann, Inorg. Chim. Acta 166 (1989) 39–46.
[26] F. Ferrier, G. Terzian, J. Mossoyan, D. Benlian, J. Mol. Struct. 344 (1995) 189–193.
[27] W.-F. Liaw, J.-H. Lee, H.-B. Gau, C.-H. Chen, G.-H. Lee, Inorg. Chim. Acta 322 (2001) 99–105.
[28] L. Hewison, T.R. Johnson, B.E. Mann, A.J.H.M. Meijer, P. Sawle, R. Motterlini, Dalton Trans. 40 (2011) 8328–8334.
[29] K.D. Karlin, S.J. Lippard, J. Am. Chem. Soc. 98 (1976) 6951–6957.
[30] D. Sellmann, U. Reineke, J. Organomet. Chem. 314 (1986) 91–103.
[31] R. Kretschmer, G. Gessner, H. Görls, S.H. Heinemann, M. Westerhausen, J. Inorg. Biochem. 105 (2011) 6–9.
[32] V.P. Lorett Velásquez, T.M.A. Jazzazi, A. Malassa, H. Görls, G. Gessner, S.H. Heinemann, M. Westerhausen, Eur. J. Inorg. Chem. (2012) 1072–1078.
[33] A. Szakács-Schmidt, J. Kreisz, L. Markó, Z. Nagy-Magos, J. Takács, Inorg. Chim. Acta 198–200 (1992) 401–405.
[34] C.-H. Chen, Y.-S. Chang, C.-Y. Yang, T.-N. Chen, C.-M. Lee, W.-F. Liaw, Dalton Trans. (2004) 137–143.
[35] M.A. Gonzalez, N.L. Fry, R. Burt, R. Davda, A. Hobbs, P.K. Mascharak, Inorg. Chem. 50 (2011) 3127–3134.
[36] C.S. Jackson, S. Schmitt, Q.P. Dou, J.J. Kodanko, Inorg. Chem. 50 (2011) 5336–5338.
[37] L. Hewison, S.H. Crook, B.E. Mann, A.J.H.M. Meijer, H. Adams, P. Sawle, R.A. Motterlini, Organometallics 31 (2012) 5823–5834.
[38] D. Scapens, H. Adams, T.R. Johnson, B.E. Mann, P. Sawle, R. Aqil, T. Perrior, R. Motterlini, Dalton Trans. (2007) 4962–4973.
[39] L. Hewison, S.H. Crook, T.R. Johnson, B.E. Mann, H. Adams, S.E. Plant, P. Sawle, R. Motterlini, Dalton Trans. 39 (2010) 8967–8975.
[40] S. Romanski, H. Rücker, E. Stamellou, M. Guttentag, J.-M. Neudörfl, R. Alberto, S. Amslinger, B. Yard, H.-G. Schmalz, Organometallics 31 (2012) 5800–5809.
[41] A.J. Atkin, I.J.S. Fairlamb, J.S. Ward, J.M. Lynam, Organometallics 31 (2012) 5894–5902.
[42] A.J. Atkin, J.M. Lynam, B.E. Moulton, P. Sawle, R. Motterlini, N.M. Boyle, M.T. Pryce, I.J.S. Fairlamb, Dalton Trans. 40 (2011) 5755–5761.
[43] S. McLean, B.E. Mann, R.K. Poole, Anal. Biochem. 427 (2012) 36–40.
[44] P.O. Lagaditis, A.A. Mikhailine, A.J. Lough, R.H. Morris, Inorg. Chem. 49 (2010) 1094–1102.
[45] J. Weidlein, U. Müller, K. Dehnicke, Schwingungsfrequenzen I: Hauptgruppenelemente, Georg Thieme, Stuttgart, 1981.
[46] K. Nakamoto, Infrared and Raman Spectra of Inorganic and Coordination Compounds, fourth ed., John Wiley, New York, 1986.
[47] J.A.S. Howell, J.-Y. Saillard, A. de Beuze, G. Jaouen, J. Chem. Soc. Dalton Trans. (1982) 2533–2537.
[48] K.R. Seipel, Z.H. Platt, M. Nguyen, A.W. Holland, J. Org. Chem. 73 (2008) 4291–4294.
[49] COLLECT, Data Collection Software, Nonius B.V, Netherlands, 1998.
[50] Z. Otwinowski, W. Minor, in: C.W. Carter, R.M. Sweet (Eds.), Methods in Enzymology, Macromolecular Crystallography, Part A, vol. 276, Academic Press, 1997, pp. 307–326.
[51] G.M. Sheldrick, Acta Crystallogr. A64 (2008) 112–122.